Human Brain Mapping

WILEY

RESEARCH ARTICLE OPEN ACCESS

Neuropathological Correlates of Volume and Shape of Deep Gray Matter Structures in Community-Based Older Adults

Khalid Saifullah[1] | Nazanin Makkinejad[1] | Md Tahmid Yasar[1] | Arnold M. Evia[2] | Sue E. Leurgans[2] | David A. Bennett[2] | Julie A. Schneider[2] | Konstantinos Arfanakis[1,2,3]

[1]Department of Biomedical Engineering, Illinois Institute of Technology, Chicago, Illinois, USA | [2]Rush Alzheimer's Disease Center, Rush University Medical Center, Chicago, Illinois, USA | [3]Department of Diagnostic Radiology and Nuclear Medicine, Rush University Medical Center, Chicago, Illinois, USA

Correspondence: Konstantinos Arfanakis (konstantinos_arfanakis@rush.edu)

Received: 27 September 2024 | **Revised:** 24 April 2025 | **Accepted:** 19 June 2025

Funding: This work was supported by National Institute of Neurological Disorders and Stroke, U01NS100599; National Institute on Aging, P30AG010161, P30AG072975, R01AG015819, R01AG017917, R01AG056405, R01AG064233, R01AG067482.

Keywords: brain | MRI | pathology | shape | volume

ABSTRACT

Age-related neurodegenerative and cerebrovascular neuropathologies often coexist in the brain of older adults and contribute to brain abnormalities, cognitive decline and dementia. While deep gray matter structures are implicated early and/or strongly in these processes, the independent effects of various age-related neuropathologies on these structures remain poorly understood. The goal of this study was to investigate the independent association of various age-related neuropathologies with the volume and shape of deep gray matter structures in a large number of community-based older adults that came to autopsy. Cerebral hemispheres from 842 participants of four community studies at the Rush Alzheimer's Disease Center were imaged with MRI ex vivo and underwent detailed neuropathologic examination. Linear regression was used to study the association of various neuropathologies with the volume and shape of six deep gray matter structures (hippocampus, amygdala, caudate, thalamus, nucleus accumbens, putamen) controlling for age at death, sex, years of education, scanner, and postmortem intervals. Both the volumetric and shape analyses showed independent associations of tangles with structural abnormalities in all deep brain structures, of limbic-predominant age-related TDP-43 encephalopathy neuropathological change (LATE-NC) with hippocampus and amygdala, of atherosclerosis with hippocampus, and of gross infarcts with caudate (all $p < 0.05$ corrected for multiple comparisons). Shape analysis revealed the corresponding independent spatial patterns of inward deformation and also showed additional associations of neuropathologies with deep brain structures ($p < 0.05$ corrected for multiple comparisons). When analyses were repeated in left and right hemispheres separately, the results were mostly similar in both hemispheres. Mixed pathologies are very common in the older adult brain and the present comprehensive study disentangles their independent effects on multiple deep gray matter structures. These neuropathologic signatures may potentially be used in combination with other features toward in vivo prediction of neuropathologies which could have important implications in future clinical trials and the development of prevention and treatment strategies.

Abbreviations: AD, Alzheimer's disease; CAA, cerebral amyloid angiopathy; LATE-NC, limbic-predominant age-related TDP-43 encephalopathy neuropathological change; NFT, neurofibrillary tangles; TDP-43, transactive response DNA-binding protein 43.

Summary

- This study investigated the independent association of various age-related neuropathologies with the volume and shape of deep gray matter structures in older adults.
- Tangles, LATE-NC, atherosclerosis, and gross infarcts were independently associated with structural abnormalities in deep brain structures.
- The results were mostly similar in left and right hemispheres but few findings were stronger in one hemisphere than the other.

1 | Introduction

Age-related neuropathologies are often mixed in the brain of older adults, have devastating effects on brain tissue, and contribute to cognitive decline and dementia (Dallaire-Théroux et al. 2017; Habes et al. 2020; Kapasi et al. 2020). Although different neurodegenerative and cerebrovascular pathologies have different patterns of accumulation in the brain, there is ample evidence that deep gray matter structures are involved early and/or are heavily burdened in the course of certain age-related pathologies through the brain (Mirra et al. 1991; Nagy et al. 1998; Thal et al. 2002; McKeith et al. 2005; Soontornniyomkij et al. 2010; Vinters et al. 2000; Amador-Ortiz and Dickson 2008; Nag et al. 2018). For example, the hippocampus and amygdala are only some of the deep gray matter structures that are known to be impacted early and heavily by Alzheimer's pathology and limbic-predominant age-related TDP-43 encephalopathy neuropathological change (LATE-NC). Magnetic resonance imaging (MRI) has been used to assess the volume and shape of deep gray matter structures and to identify structural abnormalities associated with brain pathology (Frisoni et al. 2010; Klöppel et al. 2012). Numerous studies have shown links between Alzheimer's dementia/biomarkers/pathology and atrophy of the hippocampus (Gerardin et al. 2009; Lindberg et al. 2012; Scher et al. 2007; Dawe et al. 2011; Marquié et al. 2017; Valdés Hernández et al. 2017; Tang et al. 2014; Qiu et al. 2009), amygdala (Makkinejad et al. 2019; Tang et al. 2014; Qiu et al. 2009), caudate (Al-Shaikhli et al. 2016; de Jong et al. 2011; Tang et al. 2014; Qiu et al. 2009), thalamus (Tang et al. 2014; Qiu et al. 2009), accumbens (de Jong et al. 2011), and putamen (de Jong et al. 2011; Tang et al. 2014; Qiu et al. 2009). However, Alzheimer's pathology is in most cases mixed with other neurodegenerative and/or cerebrovascular pathologies which can only be diagnosed at autopsy, and which may affect the same deep gray matter structures. This issue of mixed pathologies is true for several pathologies, not just Alzheimer's (Kapasi et al. 2017). Therefore, in order to assess the independent effects of different pathologies on the volume and shape of deep gray matter structures assessed by MRI it is necessary to know which other pathologies are present in each brain, and to control for them in analyses. To our knowledge, there is no report in the literature on the neuropathological correlates of the volume and shape of older adult deep gray matter structures that considered the effects of multiple age-related neuropathologies and studied multiple deep gray matter structures.

The purpose of this work was to disentangle the independent effects of age-related neuropathologies on the volume and shape of multiple deep gray matter structures by combining ex vivo MRI and detailed pathology data in a large number of community-based older adults. We hypothesized that a higher burden of neuropathologies is associated with lower volume and inward deformation of deep gray matter structures. The brain structures that were investigated were the nucleus accumbens, amygdala, hippocampus, caudate, putamen, and thalamus. A comprehensive list of age-related neuropathologies was considered, including neurofibrillary tangles and amyloid plaques (Kapasi et al. 2021), LATE-NC (Nelson et al. 2019), Lewy bodies (Agrawal et al. 2021), gross and microscopic infarcts (Arvanitakis et al. 2017), atherosclerosis (Arvanitakis et al. 2016), arteriolosclerosis, and cerebral amyloid angiopathy (CAA) (Boyle et al. 2015). The independent association of each of these neuropathologies with the volume and shape of each deep gray matter structure was tested, controlling for all other pathologies, demographics, and covariates in a large number of community-based older adults.

2 | Methods

2.1 | Study Population

Older adults enrolled in four longitudinal clinical-pathologic cohort studies of aging, the Rush University Memory and Aging Project (MAP), the Religious Orders Study (ROS) (Bennett et al. 2018), the Minority Aging Research Study (MARS) (Barnes et al. 2012), and the Clinical Core (CC) of the Rush Alzheimer's Disease Research Center (Barnes et al. 2015) were included in this investigation. All studies were approved by an institutional review board of Rush University Medical Center. Participants provided written informed consent and signed an anatomical gift act. Annual clinical evaluation including cognitive function testing, medical history, and neurologic examination was performed on all participants. Alzheimer's dementia was diagnosed based on the criteria of the National Institute of Neurological and Communicative Disorders and Stroke and the Alzheimer's Disease and Related Disorders Association (McKhann et al. 1984). Participants who had cognitive impairment but did not meet the criteria for dementia were classified as having mild cognitive impairment (MCI) (Bennett et al. 2002; Boyle et al. 2006). Participants with neither dementia nor MCI were classified as no cognitive impairment (NCI) (Bennett et al. 2006). At the time of these analyses, 5067 participants of the parent studies had completed the baseline clinical evaluation. Of these, 620 died and 123 withdrew from the studies before the ex vivo MRI sub-study began. Of the remaining 4324 persons, 1593 died, 1290 were autopsied, and 1039 had ex vivo MRI and pathology data. The first 856 consecutive participants with ex vivo MRI and pathology data were considered in this study, of whom 14 were excluded due to widespread brain abnormalities (e.g., large infarcts, tumors) or frontotemporal lobar degeneration. Analyses were conducted in the remaining 842 participants.

2.2 | Brain Hemisphere Preparation

At autopsy, the brain was removed and the cerebrum was separated from the cerebellum and brainstem. The cerebrum was divided into the left and right hemispheres, and the hemisphere with more visible pathology was selected for ex vivo MRI and pathologic examination, while the contralateral hemisphere was frozen and stored. The selected hemisphere was immersed in phosphate-buffered 4% formaldehyde solution and refrigerated at 4°C, within 30 min of removal from the skull. Ex vivo MRI was conducted while the hemisphere was immersed in formaldehyde solution with its medial aspect facing the bottom of an MR-compatible container, at room temperature. Gross examination was performed within 2 weeks after ex vivo MRI, followed by histopathologic diagnostic examination by a board-certified neuropathologist (Kotrotsou et al. 2015).

2.3 | Ex Vivo MRI Data Acquisition and Pre-Processing

Ex vivo MRI data were collected on four 3 Tesla MRI scanners using a two-dimensional multi-echo spin-echo sequence and the same acquisition voxel size across scanners, 0.6 mm × 0.6 mm × 1.5 mm (Arfanakis et al. 2020): General Electric Signa, TEs = 13, 52 ms, TR = 3600 ms, repetitions = 6, scan time = 31 min; Siemens Trio, TEs = 11, 33, 55 ms, TR = 3600 ms, repetitions = 4, scan time = 30.3 min; Philips Achieva, TEs = 16.5, 33, 50, 66, 83 ms, TR = 4055 ms, repetitions = 2, scan time = 35 min; Siemens Verio, TEs = 22, 33, 55 ms, TR = 3750 ms, repetitions = 4, scan time = 32 min. Only T_2-weighted images collected at similar echo times (50–55 ms) were used in this work to ensure consistent image contrast. A multi-atlas segmentation approach developed in-house was used to segment seven deep gray matter structures in the ex vivo T_2-weighted images: nucleus accumbens, amygdala, caudate, hippocampus, pallidum, putamen, and thalamus (Kotrotsou et al. 2014). All segmentations were visually inspected. Pallidum segmentation was deemed unstable due to the lack of sufficient contrast in that structure and was therefore not considered in analyses (Visser et al. 2016). The volume of each segmented structure was calculated for each participant. Rigid-body registration (FSL FLIRT, FMRIB, Oxford, UK) (Smith et al. 2004) was used to register the T_2-weighted images of each participant to an ex vivo MRI cerebral hemisphere template developed in-house, and the resulting transformations were applied to masks of the participant's segmented deep brain structures. The resulting alignment of the mask of each deep brain structure was further improved through additional rigid-body registration to the corresponding structure of the template.

2.4 | Shape Analysis

Shape analysis was carried out using the spherical harmonic basis function toolbox SPHARM-PDM (Styner et al. 2006). For each participant, the rigidly transformed mask of each deep brain structure was smoothed. A triangulated mesh was generated on the surface of each mask, and the mesh was mapped to a sphere using an area preserving and distortion minimizing algorithm. A spherical harmonic degree of 15 was chosen in SPHARM-PDM. The spherical parameterization was then sampled, and triangulated meshes were generated for the nucleus accumbens and amygdala using 1002 vertices, for the thalamus, hippocampus, and putamen with 1442 vertices, and for the caudate with 2252 vertices (different numbers of vertices were selected for different structures due to their different sizes). For each deep brain structure, the difference vector between each vertex on the average mesh and the corresponding vertex on a participant's mesh was computed. Then, each difference vector was projected to the normal vector on the corresponding vertex of the average mesh to obtain a signed local shape difference of a participant's deep brain structure from the average shape. The signed shape differences indicated that a participant's structure was locally smaller (negative) or larger (positive) relative to the corresponding average shape and were used in analyses.

2.5 | Neuropathologic Evaluation

After completion of ex vivo MRI, each hemisphere underwent detailed neuropathologic examination by a board-certified neuropathologist blinded to all imaging and clinical data, following well-established procedures (Schneider et al. 2003). Each hemisphere was sectioned into 1-cm thick coronal slabs and was macroscopically evaluated. Tissue blocks were dissected, embedded in paraffin, sectioned at 6 μm thickness, and mounted onto glass slides. Aβ and neurofibrillary tangles were identified by molecularly specific immunohistochemistry (3 monoclonal antibodies against Aβ, 4G8, 6F/3D, 10D5; antibodies to abnormally phosphorylated Tau protein, AT8) in 20 μm sections from eight brain regions (hippocampus, entorhinal, inferior temporal, angular gyrus, calcarine, anterior cingulate, superior frontal, midfrontal cortices). Regions of interest were manually outlined using Stereo Investigator software. The systematic random sampling grid within the software was applied to the regions of interest, and images at each sampling grid were manually taken. Using ImageJ software, a percentage of amyloid positivity was calculated using a custom positive-pixel algorithm. Neurofibrillary tangles were manually counted, and the count was normalized by the area. Both measures were square root transformed to generate composite measures of Aβ burden and tangle density (continuous variables) (Kapasi et al. 2021). A pathologic diagnosis of AD was also made using the National Institute on Aging-Alzheimer's Association (NIA-AA) criteria (Hyman et al. 2012) (only used in tables; analyses included the continuous variables of Aβ burden and tangle density). LATE-NC was graded into four stages: no TDP-43 inclusions (stage 0); TDP-43 inclusions in amygdala only (stage 1); TDP-43 inclusions in amygdala and entorhinal cortex or hippocampus (stage 2); TDP-43 inclusions in amygdala, entorhinal cortex or hippocampus, and neocortex (stage 3) (Nelson et al. 2019). Lewy bodies were assessed in seven regions (entorhinal, anterior cingulate, midfrontal, superior or middle temporal, and inferior parietal cortices, substantia nigra, and amygdala) and were rated as present (1) or absent (0) (Agrawal et al. 2021). Gross infarcts of any age were rated as none (0), one (1), or more than one (2). Microscopic infarcts were identified from

a minimum of nine regions (midfrontal, middle temporal, entorhinal, hippocampal, inferior parietal, and anterior cingulate cortices, anterior basal ganglia, thalamus, and midbrain) and were rated as none (0), one (1), or more than one (2) (Arvanitakis et al. 2017). Atherosclerosis was assessed at the circle of Willis and was rated as none (0), mild (1), moderate (2), or severe (3) (Arvanitakis et al. 2016). Assessment of arteriolosclerosis was done in sections of the anterior basal ganglia and was rated as none (0), mild (1), moderate (2), or severe (3). CAA was assessed in four regions (angular gyrus, midfrontal, middle temporal and calcarine cortices) and was rated as none (0), mild (0), moderate (2), and severe (3) (Boyle et al. 2015).

2.6 | Statistical Analysis

Linear regression was used to test the hypothesis that a lower volume of each deep brain structure separately (dependent variable) is associated with a higher burden of neuropathologies (independent variables) (Aβ burden, tangle density, LATE-NC stage, the presence of Lewy bodies, the ordinal variables for gross and microscopic infarcts, the severity of atherosclerosis, arteriolosclerosis, and CAA), controlling for age at death, sex, years of education, scanner, postmortem interval to immersion in formaldehyde solution, and postmortem interval to ex vivo MRI. Age at death, sex, and years of education were included as covariates due to their well-established links to brain structure and neuropathology (Baumgart et al. 2015; Nebel et al. 2018; Bennett et al. 2005), and variables for MRI scanners and postmortem intervals were included due to their effects on ex vivo MRI measurements (Hedges et al. 2022; Orlhac et al. 2022; Dawe et al. 2009). Standardized regression coefficients (β coefficients) were obtained by z-scoring the dependent and independent variables used in the linear regression model. The analysis was conducted using PALM (FSL, FMRIB, Oxford, UK) (Winkler et al. 2014) with 10,000 permutations, family-wise error rate (FWER) correction, and four exchangeability blocks (one per scanner) to ensure that permutations were conducted exclusively among participants scanned on the same scanner. Associations were considered significant at a corrected $p < 0.05$.

Shape analysis for each deep brain structure used vertex-wise linear regression to test the hypothesis that more negative signed shape difference at each vertex (dependent variable) is associated with a higher burden of neuropathologies (independent variables) (Aβ burden, tangle density, LATE-NC stage, the presence of Lewy bodies, the ordinal variables for gross and microscopic infarcts, the severity of atherosclerosis, arteriolosclerosis, and CAA), controlling for age at death, sex, years of education, scanner, postmortem interval to fixation and to imaging. Standardized β coefficients were generated. The statistical analysis was conducted using PALM (FSL, FMRIB, Oxford, UK) (Winkler et al. 2014) with more than 20 times as many permutations as the number of vertices of each structure, and four exchangeability blocks as in the volume analysis. Threshold-free cluster enhancement and family-wise error rate correction were also applied. Associations were considered significant in vertices with a corrected $p < 0.05$. The above shape analysis was first conducted after right hemispheres had been mirrored to appear like left hemispheres (because one hemisphere was studied per participant), and was then repeated for left and right hemispheres separately to investigate left right asymmetric effects.

3 | Results

3.1 | Characteristics of the Participants

Among the 842 participants, 72% were female, 31% had NCI, 23% had MCI, and 46% had dementia at the last evaluation prior to death (Table 1). The mean age at death was 90 years (SD = 6 years). The mean postmortem interval to fixation was 9.9 h (SD = 8 h). Neuropathologic evaluation showed that 69% of the participants had intermediate or high AD neuropathological change, and 55% had LATE-NC (Table 2). The mean volumes of the deep brain structures ranged from approximately 0.5 cm^3 (SD = 0.1 cm^3) (accumbens) to 4 cm^3 (SD = 1 cm^3) (thalamus) per hemisphere.

3.2 | Associations of the Volume of Deep Brain Structures With Neuropathology

Volumetric analysis showed that lower volume of deep brain structures was associated with higher tangle density, Aβ, LATE-NC, atherosclerosis, and gross infarcts (FWER corrected $p < 0.05$) (Table 3). More specifically, lower hippocampal volume was associated with a higher tangle density ($\beta = -0.263$, $p < 10^{-4}$), LATE-NC stage ($\beta = -0.134$, $p < 10^{-4}$), and atherosclerosis severity ($\beta = -0.083$, $p = 0.027$). Lower amygdala volume was associated with a higher tangle density ($\beta = -0.336$, $p < 10^{-4}$), Aβ ($\beta = -0.102$, $p = 0.014$), and LATE-NC stage ($\beta = -0.127$, $p = 0.0003$). Lower volumes in caudate ($\beta = -0.200$, $p < 10^{-4}$), thalamus ($\beta = -0.152$, $p = 0.0007$), nucleus accumbens ($\beta = -0.218$, $p < 10^{-4}$), and putamen ($\beta = -0.176$, $p = 0.0002$) were also associated with a higher tangle density. Furthermore, lower volume of the caudate was also associated with more gross infarcts ($\beta = -0.092$, $p = 0.023$). The above findings were almost identical when using a binary instead of a four-level variable for LATE-NC in the analysis (see Table S1). The above findings were generally similar in the left and right hemispheres with some exceptions. Specifically, the associations of lower volume in the thalamus and putamen with a higher tangle density, and lower caudate volume with gross infarcts were stronger in the right hemisphere compared to the left (see Tables S2 and S3).

3.3 | Associations of the Shape of Deep Brain Structures With Neuropathology

Shape analysis showed unique patterns of inward deformation of deep brain structures in association with higher tangle density, LATE-NC, atherosclerosis, gross infarcts, and Lewy bodies (Figure 1; also see Figure S1). In the hippocampus, higher tangle density was linked to inward deformation across the entire structure, while higher LATE-NC stage was linked to inward deformation in the CA1 and subiculum with the most significant effect in the head of the hippocampus. Atherosclerosis was linked to inward deformation mainly in the CA1 with the most significant effect in the tail of the hippocampus. In the amygdala, higher tangle density was linked to inward deformation across the entire

TABLE 1 | Demographics, clinical characteristics, and imaging.

Characteristics	Left and right combined	Left hemisphere	Right hemisphere
N	842	459	383
Age at death, years (SD)	90.4 (6.4)	90.2 (6.3)	90.6 (6.6)
Male, *n* (%)	239 (28.3%)	142 (30.9%)	97 (25.3%)
Non-Latino White, *n* (%)	766 (91%)	422 (91.9%)	344 (89.8%)
Non-Latino Black, *n* (%)	51 (6.1%)	23 (5%)	28 (7.3%)
Latino, *n* (%)	25 (3%)	14 (3.1%)	11 (2.9%)
Education, years (SD)	15.7 (3.6)	15.8 (3.7)	15.6 (3.5)
Mild cognitive impairment[a], *n* (%)	195 (23.2%)	100 (21.8%)	95 (24.8%)
Dementia[a], *n* (%)	383 (45.5%)	219 (47.7%)	164 (42.8%)
Mini-mental State Examination[a] (MMSE), mean (SD)	19.9 (9.5)	19.4 (9.9)	20.5 (9.1)
Postmortem interval to fixation, hours (SD)	9.9 (8.1)	9.8 (8.5)	10.0 (7.6)
Postmortem interval to imaging, days (SD)	37.5 (18.1)	38.2 (20.2)	36.7 (15.3)
Accumbens, cm^3 (SD)	0.54 (0.1)	0.54 (0.1)	0.55 (0.1)
Amygdala, cm^3 (SD)	1.48 (0.4)	1.43 (0.4)	1.53 (0.3)
Caudate, cm^3 (SD)	2.95 (0.6)	2.97 (0.6)	2.92 (0.6)
Hippocampus, cm^3 (SD)	2.86 (0.7)	2.81 (0.7)	2.91 (0.7)
Putamen, cm^3 (SD)	3.82 (0.8)	3.84 (0.8)	3.79 (0.8)
Thalamus, cm^3 (SD)	4.04 (1.0)	4.03 (1.0)	4.05 (1.0)
MRI scanner, *n* (%)			
3T GE Signa, *n* (%)	82 (9.7%)	45 (9.8%)	37 (9.7%)
3T Siemens Trio, *n* (%)	85 (10.1%)	41 (8.9%)	44 (11.5%)
3T Philips Achieva, *n* (%)	291 (34.6%)	159 (34.6%)	132 (34.5%)
3T Siemens Verio, *n* (%)	384 (45.6%)	214 (46.6%)	170 (44.4%)

Abbreviation: SD, Standard deviation.
[a]Proximate to death.

structure, while higher LATE-NC stage was linked to inward deformation mainly in the centromedial and superficial subdivisions on the superior aspect of the amygdala, and also in the laterobasal and superficial subdivisions on the inferior aspect. Atherosclerosis was linked to inward deformation in all the anterior portion of the superior aspect of the amygdala and most of the laterobasal subdivision on the inferior aspect. In the caudate, higher tangle density was linked to inward deformation across all of the superior aspect of the structure, and mainly the anterior portion of the inferior aspect of the structure, while gross infarcts were linked to inward deformation mainly in the posterior of the superior aspect of the structure and somewhat in the anterior inferior side. In the thalamus, higher tangle density was linked to inward deformation in all the anterior portion of the superior aspect of the structure including the anterior, ventral, lateral, medial nuclei, and in the posterior portion of the inferior aspect of the structure, mainly in the pulvinar, geniculate and ventral posterior nuclei. Lewy bodies were linked to inward deformation mainly in the central medial, ventral lateral posterior, and ventral posterior nuclei of the thalamus. In the nucleus accumbens, higher tangle density was linked to inward deformation across almost the entire structure and higher LATE-NC stage was linked to inward deformation mainly in its superior aspect. Finally, in the putamen, higher tangle density was linked to inward deformation across almost the entire structure. The above findings were generally similar in the left and right hemispheres with some exceptions. Specifically, the associations of inward deformations in the caudate with a higher tangle density, and in the amygdala with atherosclerosis were stronger in the left hemisphere (see Figures S2 and S3), while the associations of inward deformations in the thalamus and putamen with a higher tangle density, and in the caudate with gross infarcts were stronger in the right hemisphere (see Figures S4 and S5). In addition, separate shape analyses in the right and left hemispheres showed associations of inward deformation with additional pathologies that did not show significance in the analysis considering both hemispheres at the same time. Specifically, inward deformation in the left caudate was associated with arteriolosclerosis (see Figures S2 and S3), and inward deformation of the right hippocampus, amygdala, caudate, accumbens and putamen was associated with microscopic infarcts (see Figures S4 and S5).

TABLE 2 | Neuropathologic characteristics considering all study participants.

Characteristics	Left and right combined	Left hemisphere	Right hemisphere
AD-NC (NIA-AA), *n* (%)			
High	212 (25%)	128 (28%)	84 (22%)
Intermediate	366 (44%)	205 (45%)	161 (42%)
Low	164 (20%)	72 (16%)	92 (24%)
LATE-NC, *n* (%)			
Stage 3	220 (26.1%)	132 (28.8%)	88 (23.0%)
Stage 2	94 (11.1%)	56 (12.2%)	38 (9.9%)
Stage 1	153 (18.2%)	76 (16.6%)	77 (20.1%)
Lewy bodies, *n* (%)	242 (28.7%)	139 (30.3%)	103 (26.9%)
Gross infarcts, *n* (%)	343 (40.7%)	173 (37.7%)	170 (44.4%)
Microscopic infarcts, *n* (%)	329 (39.1%)	163 (35.5%)	166 (43.3%)
Atherosclerosis, *n* (%)			
Severe	44 (5.2%)	21 (4.6%)	23 (6.0%)
Moderate	164 (19.5%)	87 (19.0%)	77 (20.1%)
Mild	439 (52.1%)	249 (54.2%)	190 (49.6%)
Cerebral amyloid angiopathy, *n* (%)			
Severe	98 (11.6%)	52 (11.3%)	46 (12.0%)
Moderate	202 (24.0%)	105 (22.9%)	97 (25.3%)
Mild	365 (43.3%)	209 (45.5%)	156 (40.7%)
Arteriosclerosis, *n* (%)			
Severe	50 (5.9%)	24 (5.2%)	26 (6.8%)
Moderate	174 (20.7%)	101 (22.0%)	73 (19.1%)
Mild	325 (38.6%)	167 (36.4%)	158 (41.3%)

Abbreviations: AD-NC, Alzheimer's disease neuropathologic change; LATE-NC, Limbic-predominant age-related TDP-43 encephalopathy neuropathological change; NIA-AA, National Institute on Aging-Alzheimer's Association.

4 | Discussion

The present study investigated the independent effects of age-related neuropathologies on the volume and shape of multiple deep gray matter structures by combining ex vivo MRI and detailed pathology data in a large number of community-based older adults. We hypothesized that a higher burden of neuropathologies is associated with lower volume and inward deformation of deep gray matter structures. Both the volumetric and shape analyses showed independent associations of tangles with structural abnormalities in all deep brain structures, of LATE-NC with the hippocampus and amygdala, of atherosclerosis with the hippocampus, and of gross infarcts with the caudate. Shape analysis further revealed the corresponding independent spatial patterns of inward deformation and also showed additional associations of LATE-NC with inward deformation in part of the nucleus accumbens, of atherosclerosis with part of the amygdala, and of Lewy bodies with a portion of the thalamus. When all analyses were repeated in the left and right hemispheres separately, the results were generally similar across hemispheres, but it was shown that the associations of tangles with the thalamus and putamen, and gross infarcts with the caudate were more pronounced in the right hemisphere, while the associations of tangles with the caudate and atherosclerosis with the amygdala were stronger in the left hemisphere. While numerous studies have shown links between mainly Alzheimer's pathology and atrophy of deep gray matter structures, the present study provides important new information on the independent effects of multiple neuropathologies on both the volume and shape of multiple deep gray matter structures, an important contribution considering that mixed pathologies are very common and the present study disentangles their effects.

4.1 | Tangles

Both volumetric and shape analyses showed that higher tangle density was independently associated with less tissue in all deep brain structures. These findings are in good agreement with previous studies combining MRI volumetry/morphometry with pathology (Whitwell et al. 2008) or clinical assessments (Cho et al. 2013;

TABLE 3 | Associations of the volume of deep brain structures with neuropathologies considering all 842 hemispheres and controlling for demographics, scanners and postmortem intervals to fixation and to ex vivo MRI.

	Aβ β (*p*)	Tangle density β (*p*)	LATE-NC β (*p*)	Lewy bodies β (*p*)	Gross infarcts β (*p*)	Micro infarcts β (*p*)	Athero-sclerosis β (*p*)	Arteriolosclerosis β (*p*)	CAA β (*p*)
Hippocampus	−0.068 (0.12)	**−0.263** (**$<10^{-4}$**)	**−0.134** (**$<10^{-4}$**)	−0.024 (0.55)	−0.014 (0.75)	−0.018 (0.66)	**−0.083** (**0.027**)	0.020 (0.98)	−0.022 (0.61)
Amygdala	**−0.102** (**0.0137**)	**−0.336** (**$<10^{-4}$**)	**−0.127** (**0.0003**)	−0.024 (0.55)	0.018 (0.98)	−0.029 (0.50)	−0.057 (0.17)	0.017 (0.97)	0.030 (0.99)
Caudate	−0.003 (0.87)	**−0.200** (**$<10^{-4}$**)	0.004 (0.91)	0.022 (0.98)	**−0.092** (**0.023**)	−0.013 (0.76)	0.038 (0.99)	0.037 (0.99)	−0.019 (0.68)
Thalamus	−0.031 (0.62)	**−0.152** (**0.0007**)	−0.033 (0.51)	−0.053 (0.24)	−0.069 (0.14)	−0.013 (0.77)	−0.013 (0.79)	−0.029 (0.60)	−0.006 (0.83)
Accumbens	−0.036 (0.50)	**−0.218** (**$<10^{-4}$**)	−0.051 (0.21)	−0.001 (0.87)	0.030 (0.99)	−0.027 (0.55)	0.007 (0.93)	−0.005 (0.84)	0.011 (0.95)
Putamen	−0.003 (0.87)	**−0.176** (**0.0002**)	−0.047 (0.34)	0.066 (1.00)	−0.033 (0.54)	−0.030 (0.56)	0.024 (0.98)	0.074 (1.00)	−0.058 (0.24)

Note: *p*-values are FWER-corrected. Significant findings ($p < 0.05$) are presented in bold font. Standardized beta coefficients (β) are shown.
Abbreviations: CAA, Cerebral amyloid angiopathy; LATE-NC, Limbic-predominant age-related TDP-43 encephalopathy neuropathological change.

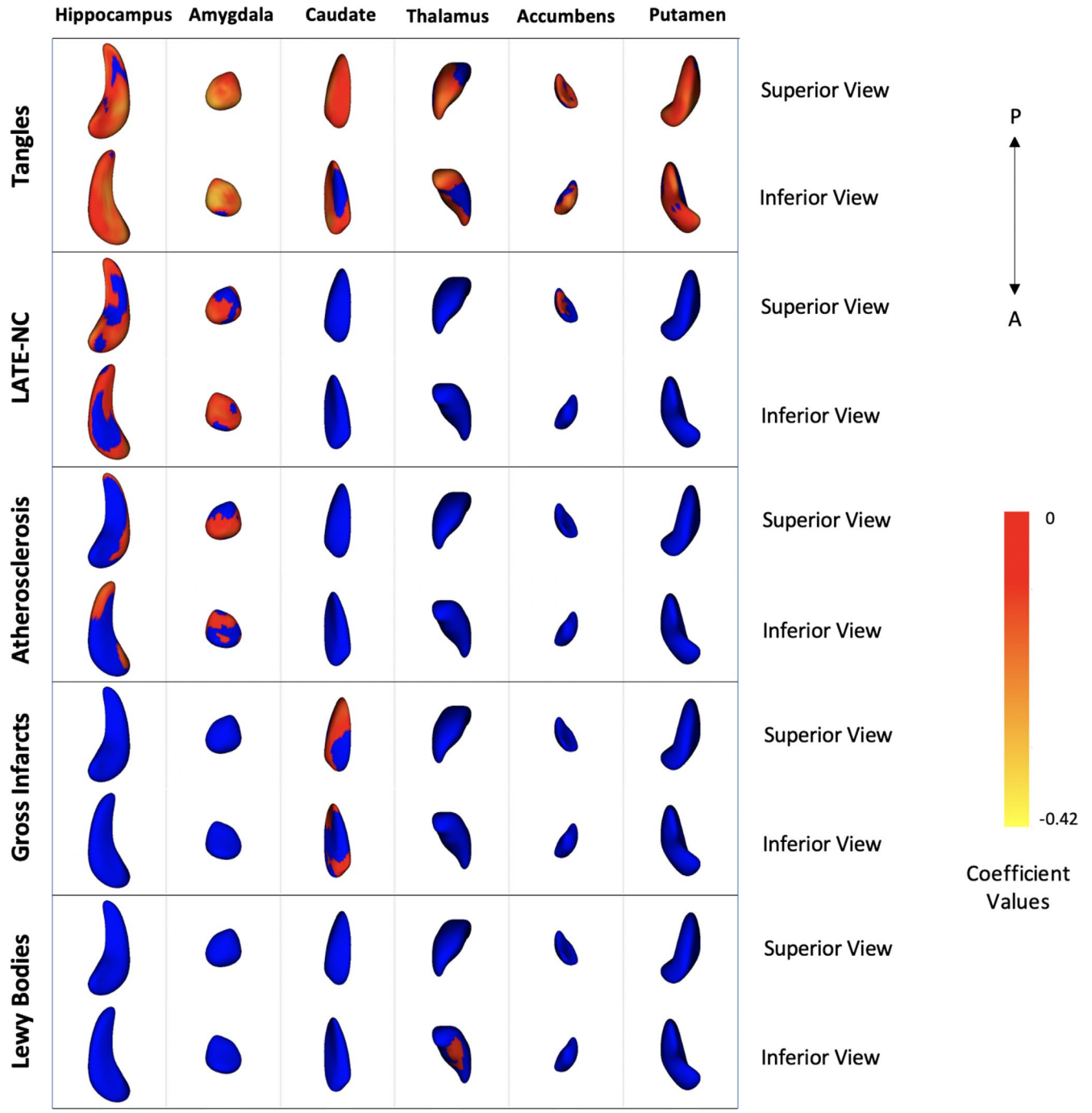

FIGURE 1 | Surface rendering of deep brain structures showing at each vertex the standardized regression coefficient for the association of the signed shape difference with various neuropathologies. This analysis considered both left and right hemispheres after mirroring right hemispheres to look like left. Red-yellow colors are assigned to vertices with significant (FWER-corrected $p < 0.05$) negative coefficients representing inward deformation, while blue colors represent no significant inward deformation. This figure shows superior and inferior views of the structures. Medial and lateral views of the same results can be found in the (Figure S1).

Roh et al. 2011; Yi et al. 2016), and can be explained by the well-established link between tangles and neuronal loss (DeTure and Dickson 2019). Furthermore, the finding that tangles was the only pathology that was associated with lower volume in all deep brain structures is consistent with the strong impact of tangles on cognition (Nelson et al. 2007; Fonseca et al. 2024).

In the hippocampus, shape analysis showed that higher tangle density was independently associated with inward deformation across the entire structure. This hippocampus-wide association is in general agreement with previous studies that combined MRI with pathology (Dawe et al. 2011; Hanko et al. 2019) or clinical diagnosis (Chan et al. 2001; Chapleau et al. 2020), as well as with the known distribution of tangles along the hippocampus (Furcila et al. 2019; Yushkevich et al. 2021). In contrast, one study on individuals with intermediate to high levels of Alzheimer's neuropathology demonstrated association of tau only with the posterior hippocampus, but that may be due

to that study's small sample size, limited range of Alzheimer's neuropathology severity, and use of in vivo MRI with relatively long antemortem intervals which leads to an underestimation of effects (de Flores et al. 2020). The present study also showed that the association of tangle density with volume and shape was rather similar in left and right hippocampi with only a slightly stronger effect in the left hippocampus, in agreement with previous work combining MRI and clinical diagnosis (Shi et al. 2009).

In the amygdala, shape analysis showed that higher tangle density was independently associated with inward deformation across the entire structure, in agreement with (Herzog and Kemper 1980) who showed significant decline in cell-packing density in all amygdala subdivisions in Alzheimer's. The largest inward deformation was observed in the laterobasal subdivision which is consistent with previous findings based on histopathology (Braak and Braak 1991; Scott et al. 1991; Makkinejad et al. 2019) or clinical diagnosis (Qiu et al. 2009; Miller et al. 2015). The laterobasal subdivision of the amygdala has strong connections to the hippocampus and entorhinal cortex (Pikkarainen et al. 1999; Pitkänen et al. 2002), and therefore the present findings suggest an important role of this region in Alzheimer's.

Caudate and putamen also showed patterns of inward deformation with higher tangle density in agreement with an early study (Mann 1991). Deformation in the caudate was observed on most of the structure's surface, especially on the head of the caudate (Whitwell et al. 2008) which is involved in emotional and affective aspects of behavior such as reward processing (Graff-Radford et al. 2017), while the rest of the caudate is involved in cognitive and executive functions such as spatial working memory (Graff-Radford et al. 2017). The association with a higher tangle density in the left caudate was stronger than that in the right caudate. Deformation in the putamen, which is involved in different types of learning and motor control, reward, emotional processing, and addiction (Luo et al. 2019), was observed almost across the entire structure, and it was the right putamen that showed stronger association of inward deformation with a higher tangle density. The thalamus showed inward deformation in both posterior and anterior portions that are crucial for visual and auditory processing, relaying sensory and motor information, memory, emotions, behavior regulation, attention, and planning (Fama and Sullivan 2015). The right thalamus showed a more pronounced association of inward deformation with a higher tangle density. Inward deformation in the nucleus accumbens in association with higher tangle density was observed across most of the structure. The nucleus accumbens has connections to the hippocampus, amygdala, thalamus, and the prefrontal cortex and is involved in pleasure, reward, addiction, and pain (Harris and Peng 2020). Previous work combining MRI and clinical diagnosis has shown inward deformation of the nucleus accumbens in patients with AD (Nie et al. 2017).

4.2 | LATE-NC

Both volumetric and shape analyses showed that LATE-NC was independently associated with less tissue in the hippocampus and amygdala. These two structures are typically involved first in the progression of LATE-NC (Nelson et al. 2023). In the hippocampus, inward deformation was observed mainly on the head, but also in CA1/subiculum and tail portions. A previous ex vivo MRI and pathology study on hippocampal sclerosis, which is often considered an end stage of LATE-NC, showed a very similar pattern of inward deformation (Dawe et al. 2011). Predominantly anterior hippocampal atrophy and hypometabolism have been reported by others (Bejanin et al. 2019; Buciuc et al. 2020; de Flores et al. 2020; Teipel et al. 2020). In the amygdala, inward deformation was observed in the centromedial, superficial, and laterobasal subdivisions. The laterobasal subdivision connects the amygdala to the hippocampus and entorhinal cortex, which is consistent with the memory deficits associated with LATE-NC (Wilson et al. 2013). The superficial subdivision has connections to the olfactory bulb (Price 2003), and the centromedial subdivision has connections to the orbital and medial prefrontal cortex, brainstem, insula, and hypothalamus. Our findings in the amygdala are in good agreement with a previous ex vivo MRI and pathology study with manual segmentation of the amygdala but included a smaller sample size (Makkinejad et al. 2019). Shape analysis also showed inward deformation of the nucleus accumbens in association with LATE-NC, but volumetric analysis did not show significantly lower volume. This is most likely due to the higher sensitivity of shape analysis in detecting localized abnormalities, combined with the potentially small effect of such abnormalities on the total volume of the structure and not sufficient power to detect it with volumetric analysis.

4.3 | Atherosclerosis

Both volumetric and shape analyses showed that atherosclerosis was independently associated with less tissue in the hippocampus. This may be a result of lower blood flow to the hippocampus and is consistent with the cognitive deficits associated with atherosclerosis, which include lower episodic and semantic memory as well as lower perceptual speed and visuospatial abilities (Arvanitakis et al. 2016). A recent ex vivo MRI volumetry and pathology study also showed the association of intracranial atherosclerosis with lower hippocampal volume and further demonstrated that this association was attenuated at higher age or at higher systolic blood pressure (Kapasi et al. 2024). In contrast, an earlier study that combined in vivo MRI and pathology did not detect any significant association with hippocampal volume, most likely due to a small sample size (Jagust et al. 2008). A novel finding of the shape analysis in the present study was that atherosclerosis-related inward deformation of the hippocampus was located mainly in the tail and body of the hippocampus. This is consistent with previous work showing that the posterior portion of the hippocampus is involved in space processing and retrieval of spatial memory (Strange et al. 2014) and the cognitive domains most strongly impaired with atherosclerosis are perceptual speed and visuospatial abilities (Arvanitakis et al. 2016). Shape analysis also showed inward deformation of the amygdala in association with atherosclerosis, but volumetric analysis did not show significantly lower volume. This is most likely due to the higher sensitivity of shape analysis in detecting localized abnormalities.

4.4 | Gross Infarcts

Both volumetric and shape analyses showed that gross infarcts were independently associated with less tissue in the caudate, and the association in the right caudate was stronger than that in the left. In fact, gross infarcts were the only cerebrovascular pathology that was linked to the caudate, and the only other age-related neuropathology associated with less tissue in the caudate was tangles. Since the caudate plays an important role in executive functions such as spatial working memory (Graff-Radford et al. 2017) the findings of the present study may offer support for previous studies showing that gross infarcts are among the few vascular pathologies that are associated with declines in working memory and visuospatial abilities (Lamar et al. 2022).

4.5 | Lewy Bodies

Lewy bodies were independently linked to inward deformation mainly in the inferior aspect of the thalamus in the central medial, ventral lateral posterior, and ventral posterior nuclei. The thalamus plays important roles in movement control, attention, executive function, and memory, and the specific nuclei implicated in the present study have known connections to the somatosensory, striate, and extrastriate cortex, among others (Fama and Sullivan 2015). Thus, the findings of the present work are in line with some of the main clinical features of Lewy bodies, which include parkinsonism, visuospatial dysfunction, and hallucinations, among others (Donaghy and McKeith 2014). Previous studies on brain atrophy in patients with Lewy body dementia reported findings with apparently little overlap across studies and involved a variety of regions including the thalamus, substantia innominata, hypothalamus, midbrain, temporal lobes, and cerebellum (Caso et al. 2021; Yoo et al. 2020; Kantarci et al. 2012; Oppedal et al. 2019; Whitwell et al. 2007). This variability may have been due to small sample sizes, use of clinical diagnosis instead of pathology, and inability to control for other pathologies. Nevertheless, the thalamus has strong connections to all of these regions that were previously reported in patients with Lewy body dementia, suggesting that the findings of the present study may bridge these otherwise disparate results. While shape analysis showed inward deformation of the thalamus in association with Lewy bodies, in volumetric analysis, the association with lower volume of the thalamus did not reach significance. This is probably due to the higher sensitivity of shape analysis in detecting localized abnormalities.

4.6 | Other Pathologies

Separate shape analyses exclusively in right or left hemispheres showed additional associations of inward deformation in the left caudate with arteriolosclerosis, and in the right hippocampus, amygdala, caudate, accumbens, and putamen with microscopic infarcts, but these findings were not present in the analysis considering both hemisphere sides at the same time. Small vessel disease is known to affect subcortical brain tissue and deep brain structures (van Veluw et al. 2022). However, the single hemisphere side analyses had approximately half the sample size of the main analysis, which was based on both sides, and therefore the additional findings from the single hemisphere side analyses require further investigation and validation. Finally, volumetric analysis considering all hemispheres showed that Aβ burden was independently associated with less tissue in the amygdala, and the same was true in the right hemispheres. This finding may indicate a residual effect of Alzheimer's pathology on the amygdala that was not captured by our tangle density metric.

4.7 | Strengths and Limitations

The present study has major strengths and some limitations. First, the combination of high-quality MRI and detailed pathology data in a large number of older adults made it possible to investigate the independent effects of neuropathologies on deep gray matter structures. Second, the inclusion of community-based older adults enhances the generalization of findings. Third, multiple structures were considered in the same study as opposed to single or few, providing a global picture of the associations of pathology with structure in deep gray matter. Fourth, ex vivo MRI has multiple advantages over in vivo MRI in studies combining MRI and pathology (e.g., no additional pathology developing after imaging and before autopsy, no bias toward less frail individuals), and the results are expected to translate well to in vivo since we have previously demonstrated that a linear relationship exists between structural brain information collected ex vivo and in vivo on the same individuals (Kotrotsou et al. 2014). One limitation of the present study is that only one hemisphere was available from each participant and there were 17% fewer right hemispheres than left, slightly lowering the power of analyses in the right hemisphere. Another limitation is that the participants were on average older than those in typical in vivo aging studies because this study requires pathology information that is available only at autopsy. In addition, 91% of the participants were non-Latino White, and future studies are needed to replicate the findings in other racial and ethnic groups. Finally, volume and shape metrics were not normalized by intracranial volume as the ex vivo images did not include the skull. Nevertheless, normalizing by height, which has previously been used as a surrogate for head size, did not change the conclusions of this work. Also, the large sample size largely alleviates any potential biases due to head size.

4.8 | Future Research

Future research combining in vivo MRI with short antemortem intervals and autopsy in a large number of community-based older adults will aim to validate the present findings in living persons, will allow more thorough investigation of laterality because both hemispheres will be imaged on each participant, may provide insight on the association of neuropathologies with the rate of change in volume and shape of deep brain structures proximal to death assuming longitudinal imaging, and depending on the MRI modalities used will allow investigation of the association of neuropathologies with other characteristics of deep brain structures that cannot be measured ex vivo, for example, perfusion. Furthermore, future research will test to what degree volume and shape abnormalities in deep gray matter structures

mediate the relation of age-related neuropathologies with cognitive and motor outcomes.

5 | Conclusion

The present study revealed the independent effects of age-related neuropathologies on both the volume and shape of multiple deep gray matter structures by combining ex vivo MRI and detailed pathology data in a large number of community-based older adults. The importance of this contribution lies in the fact that mixed pathologies are very common and the present study disentangles their effects on multiple deep gray matter structures. Although some overlap was observed in the signatures of different neuropathologies on deep brain structures, there were also major differences that could potentially be utilized in combination with other features toward in vivo prediction of certain age-related neuropathologies. This could have important implications in future clinical trials, and in the development of prevention and treatment strategies.

Acknowledgments

The authors would like to thank the participants and staff of the Rush University Memory and Aging Project (MAP), the Religious Orders Study (ROS), the Minority Aging Research Study (MARS), and the Clinical Core (CC) of the Rush Alzheimer's Disease Research Center. This study was supported by the following grants from the National Institutes of Health: R01AG064233, R01AG067482, R01AG017917, R01AG015819, R01AG056405, P30AG010161, P30AG072975 (National Institute on Aging), and U01NS100599 (National Institute of Neurological Disorders and Stroke).

Conflicts of Interest

The authors declare no conflicts of interest.

Data Availability Statement

The data that support the findings of this study are available on request from the corresponding author. The data are not publicly available due to privacy or ethical restrictions.

References

Agrawal, S., L. Yu, S. Nag, et al. 2021. "The Association of Lewy Bodies With Limbic-Predominant Age-Related TDP-43 Encephalopathy Neuropathologic Changes and Their Role in Cognition and Alzheimer's Dementia in Older Persons." *Acta Neuropathologica Communications* 9, no. 1: 156. https://doi.org/10.1186/s40478-021-01260-0.

Al-Shaikhli, S. D., M. Y. Yang, and B. Rosenhahn. 2016. "Alzheimer's Disease Detection via Automatic 3D Caudate Nucleus Segmentation Using Coupled Dictionary Learning With Level Set Formulation." *Computer Methods and Programs in Biomedicine* 137: 329–339. https://doi.org/10.1016/j.cmpb.2016.09.007.

Amador-Ortiz, C., and D. W. Dickson. 2008. "Neuropathology of Hippocampal Sclerosis." *Handbook of Clinical Neurology* 89: 569–572. https://doi.org/10.1016/S0072-9752(07)01253-5.

Arfanakis, K., A. M. Evia, S. E. Leurgans, et al. 2020. "Neuropathologic Correlates of White Matter Hyperintensities in a Community-Based Cohort of Older Adults." *Journal of Alzheimer's Disease: JAD* 73, no. 1: 333–345. https://doi.org/10.3233/JAD-190687.

Arvanitakis, Z., A. W. Capuano, S. E. Leurgans, D. A. Bennett, and J. A. Schneider. 2016. "Relation of Cerebral Vessel Disease to Alzheimer's Disease Dementia and Cognitive Function in Elderly People: A Cross-Sectional Study." *Lancet Neurology* 15: 934–943. https://doi.org/10.1016/S1474-4422(16)30029-1.

Arvanitakis, Z., A. W. Capuano, S. E. Leurgans, A. S. Buchman, D. A. Bennett, and J. A. Schneider. 2017. "The Relationship of Cerebral Vessel Pathology to Brain Microinfarcts." *Brain Pathology (Zurich, Switzerland)* 27, no. 1: 77–85. https://doi.org/10.1111/bpa.12365.

Barnes, L. L., S. Leurgans, N. T. Aggarwal, et al. 2015. "Mixed Pathology Is More Likely in Black Than White Decedents With Alzheimer Dementia." *Neurology* 85, no. 6: 528–534. https://doi.org/10.1212/WNL.0000000000001834.

Barnes, L. L., R. C. Shah, N. T. Aggarwal, D. A. Bennett, and J. A. Schneider. 2012. "The Minority Aging Research Study: Ongoing Efforts to Obtain Brain Donation in African Americans Without Dementia." *Current Alzheimer Research* 9, no. 6: 734–745. https://doi.org/10.2174/156720512801322627.

Baumgart, M., H. M. Snyder, M. C. Carrillo, S. Fazio, H. Kim, and H. Johns. 2015. "Summary of the Evidence on Modifiable Risk Factors for Cognitive Decline and Dementia: A Population-Based Perspective." *Alzheimer's & Dementia: The Journal of the Alzheimer's Association* 11, no. 6: 718–726. https://doi.org/10.1016/j.jalz.2015.05.016.

Bejanin, A., M. E. Murray, P. Martin, et al. 2019. "Antemortem Volume Loss Mirrors TDP-43 Staging in Older Adults With Non-Frontotemporal Lobar Degeneration." *Brain: A Journal of Neurology* 142, no. 11: 3621–3635. https://doi.org/10.1093/brain/awz277.

Bennett, D. A., A. S. Buchman, P. A. Boyle, L. L. Barnes, R. S. Wilson, and J. A. Schneider. 2018. "Religious Orders Study and Rush Memory and Aging Project." *Journal of Alzheimer's Disease* 64: S161–S189. https://doi.org/10.3233/JAD-179939.

Bennett, D. A., J. A. Schneider, Z. Arvanitakis, et al. 2006. "Neuropathology of Older Persons Without Cognitive Impairment From Two Community-Based Studies." *Neurology* 66, no. 12: 1837–1844. https://doi.org/10.1212/01.wnl.0000219668.47116.e6.

Bennett, D. A., J. A. Schneider, R. S. Wilson, J. L. Bienias, and S. E. Arnold. 2005. "Education Modifies the Association of Amyloid but Not Tangles With Cognitive Function." *Neurology* 65, no. 6: 953–955. https://doi.org/10.1212/01.wnl.0000176286.17192.69.

Bennett, D. A., R. S. Wilson, J. A. Schneider, et al. 2002. "Natural History of Mild Cognitive Impairment in Older Persons." *Neurology* 59: 198–205.

Boyle, P. A., R. S. Wilson, N. T. Aggarwal, Y. Tang, and D. A. Bennett. 2006. "Mild Cognitive Impairment: Risk of Alzheimer Disease and Rate of Cognitive Decline." *Neurology* 67: 441–445. https://doi.org/10.1212/01.wnl.0000228244.10416.20.

Boyle, P. A., L. Yu, S. Nag, et al. 2015. "Cerebral Amyloid Angiopathy and Cognitive Outcomes in Community-Based Older Persons." *Neurology* 85, no. 22: 1930–1936. https://doi.org/10.1212/WNL.0000000000002175.

Braak, H., and E. Braak. 1991. "Neuropathological Stageing of Alzheimer-Related Changes." *Acta Neuropathologica* 82: 239–259. https://doi.org/10.1007/BF00308809.

Buciuc, M., H. Botha, M. E. Murray, et al. 2020. "Utility of FDG-PET in Diagnosis of Alzheimer-Related TDP-43 Proteinopathy." *Neurology* 95, no. 1: e23–e34. https://doi.org/10.1212/WNL.0000000000009722.

Caso, F., F. Agosta, P. G. Scamarcia, et al. 2021. "A Multiparametric MRI Study of Structural Brain Damage in Dementia With Lewy Bodies: A Comparison With Alzheimer's Disease." *Parkinsonism & Related Disorders* 91: 154–161. https://doi.org/10.1016/j.parkreldis.2021.09.025.

Chan, D., N. C. Fox, R. I. Scahill, et al. 2001. "Patterns of Temporal Lobe Atrophy in Semantic Dementia and Alzheimer's Disease." *Annals of Neurology* 49, no. 4: 433–442.

Chapleau, M., C. Bedetti, G. A. Devenyi, et al. 2020. "Deformation-Based Shape Analysis of the Hippocampus in the Semantic Variant of Primary Progressive Aphasia and Alzheimer's Disease." *NeuroImage: Clinical* 27: 102305. https://doi.org/10.1016/j.nicl.2020.102305.

Cho, H., S. W. Seo, J.-H. Kim, et al. 2013. "Changes in Subcortical Structures in Early- Versus Late-Onset Alzheimer's Disease." *Neurobiology of Aging* 34: 1740–1747. https://doi.org/10.1016/j.neurobiolaging.2013.01.001.

Dallaire-Théroux, C., B. L. Callahan, O. Potvin, S. Saikali, and S. Duchesne. 2017. "Radiological-Pathological Correlation in Alzheimer's Disease: Systematic Review of Antemortem Magnetic Resonance Imaging Findings." *Journal of Alzheimer's Disease: JAD* 57, no. 2: 575–601. https://doi.org/10.3233/JAD-161028.

Dawe, R. J., D. A. Bennett, J. A. Schneider, S. K. Vasireddi, and K. Arfanakis. 2009. "Postmortem MRI of Human Brain Hemispheres: T2 Relaxation Times During Formaldehyde Fixation." *Magnetic Resonance in Medicine* 61, no. 4: 810–818. https://doi.org/10.1002/mrm.21909.

Dawe, R. J., D. A. Bennett, J. A. Schneider, and K. Arfanakis. 2011. "Neuropathologic Correlates of Hippocampal Atrophy in the Elderly: A Clinical, Pathologic, Postmortem MRI Study." *PLoS One* 6: e26286. https://doi.org/10.1371/journal.pone.0026286.

de Flores, R., L. E. M. Wisse, S. R. Das, et al. 2020. "Contribution of Mixed Pathology to Medial Temporal Lobe Atrophy in Alzheimer's Disease." *Alzheimer's & Dementia: The Journal of the Alzheimer's Association* 16, no. 6: 843–852. https://doi.org/10.1002/alz.12079.

de Jong, L. W., L. Ferrarini, J. van der Grond, et al. 2011. "Shape Abnormalities of the Striatum in Alzheimer's Disease." *Journal of Alzheimer's Disease: JAD* 23, no. 1: 49–59. https://doi.org/10.3233/JAD-2010-101026.

DeTure, M. A., and D. W. Dickson. 2019. "The Neuropathological Diagnosis of Alzheimer's Disease." *Molecular Neurodegeneration* 14: 32. https://doi.org/10.1186/s13024-019-0333-5.

Donaghy, P. C., and I. G. McKeith. 2014. "The Clinical Characteristics of Dementia With Lewy Bodies and a Consideration of Prodromal Diagnosis." *Alzheimer's Research & Therapy* 6, no. 4: 46. https://doi.org/10.1186/alzrt274.

Fama, R., and E. V. Sullivan. 2015. "Thalamic Structures and Associated Cognitive Functions: Relations With Age and Aging." *Neuroscience and Biobehavioral Reviews* 54: 29–37. https://doi.org/10.1016/j.neubiorev.2015.03.008.

Fonseca, C. S., S. L. Baker, L. Dobyns, M. Janabi, W. J. Jagust, and T. M. Harrison. 2024. "Tau Accumulation and Atrophy Predict Amyloid Independent Cognitive Decline in Aging." *Alzheimer's & Dementia: The Journal of the Alzheimer's Association* 20, no. 4: 2526–2537. https://doi.org/10.1002/alz.13654.

Frisoni, G. B., N. C. Fox, C. R. Jack, P. Scheltens, and P. M. Thompson. 2010. "The Clinical Use of Structural MRI in Alzheimer Disease." *Nature Reviews. Neurology* 6: 67–77. https://doi.org/10.1038/nrneurol.2009.215.

Furcila, D., M. Domínguez-Álvaro, J. DeFelipe, and L. Alonso-Nanclares. 2019. "Subregional Density of Neurons, Neurofibrillary Tangles and Amyloid Plaques in the Hippocampus of Patients With Alzheimer's Disease." *Frontiers in Neuroanatomy* 13: 99. https://doi.org/10.3389/fnana.2019.00099.

Gerardin, E., G. Chételat, M. Chupin, et al. 2009. "Multidimensional Classification of Hippocampal Shape Features Discriminates Alzheimer's Disease and Mild Cognitive Impairment From Normal Aging." *NeuroImage* 47: 1476–1486. https://doi.org/10.1016/j.neuroimage.2009.05.036.

Graff-Radford, J., L. Williams, D. T. Jones, and E. E. Benarroch. 2017. "Caudate Nucleus as a Component of Networks Controlling Behavior." *Neurology* 89: 2192–2197. https://doi.org/10.1212/WNL.0000000000004680.

Habes, M., M. J. Grothe, B. Tunc, C. McMillan, D. A. Wolk, and C. Davatzikos. 2020. "Disentangling Heterogeneity in Alzheimer's Disease and Related Dementias Using Data-Driven Methods." *Biological Psychiatry* 88, no. 1: 70–82. https://doi.org/10.1016/j.biopsych.2020.01.016.

Hanko, V., A. C. Apple, K. I. Alpert, et al. 2019. "In Vivo Hippocampal Subfield Shape Related to TDP-43, Amyloid Beta, and Tau Pathologies." *Neurobiology of Aging* 74: 171–181. https://doi.org/10.1016/j.neurobiolaging.2018.10.013.

Harris, H. N., and Y. B. Peng. 2020. "Evidence and Explanation for the Involvement of the Nucleus Accumbens in Pain Processing." *Neural Regeneration Research* 15, no. 4: 597–605. https://doi.org/10.4103/1673-5374.266909.

Hedges, E. P., M. Dimitrov, U. Zahid, et al. 2022. "Reliability of Structural MRI Measurements: The Effects of Scan Session, Head Tilt, Inter-Scan Interval, Acquisition Sequence, FreeSurfer Version and Processing Stream." *NeuroImage* 246: 118751. https://doi.org/10.1016/j.neuroimage.2021.118751.

Herzog, A. G., and T. L. Kemper. 1980. "Amygdaloid Changes in Aging and Dementia." *Archives of Neurology* 37: 625–629. https://doi.org/10.1001/archneur.1980.00500590049006.

Hyman, B. T., C. H. Phelps, T. G. Beach, et al. 2012. "National Institute on Aging-Alzheimer's Association Guidelines for the Neuropathologic Assessment of Alzheimer's Disease." *Alzheimer's & Dementia: The Journal of the Alzheimer's Association* 8, no. 1: 1–13. https://doi.org/10.1016/j.jalz.2011.10.007.

Jagust, W. J., L. Zheng, D. J. Harvey, et al. 2008. "Neuropathological Basis of Magnetic Resonance Images in Aging and Dementia." *Annals of Neurology* 63: 72–80. https://doi.org/10.1002/ana.21296.

Kantarci, K., T. J. Ferman, B. F. Boeve, et al. 2012. "Focal Atrophy on MRI and Neuropathologic Classification of Dementia With Lewy Bodies." *Neurology* 79, no. 6: 553–560. https://doi.org/10.1212/WNL.0b013e31826357a5.

Kapasi, A., A. W. Capuano, M. Lamar, et al. 2024. "Atherosclerosis and Hippocampal Volumes in Older Adults: The Role of Age and Blood Pressure." *Journal of the American Heart Association* 13, no. 3: e031551. https://doi.org/10.1161/JAHA.123.031551.

Kapasi, A., C. DeCarli, and J. A. Schneider. 2017. "Impact of Multiple Pathologies on the Threshold for Clinically Overt Dementia." *Acta Neuropathologica* 134, no. 2: 171–186. https://doi.org/10.1007/s00401-017-1717-7.

Kapasi, A., S. E. Leurgans, Z. Arvanitakis, L. L. Barnes, D. A. Bennett, and J. A. Schneider. 2021. "Aβ (Amyloid Beta) and Tau Tangle Pathology Modifies the Association Between Small Vessel Disease and Cortical Microinfarcts." *Stroke* 52, no. 3: 1012–1021. https://doi.org/10.1161/STROKEAHA.120.031073.

Kapasi, A., L. Yu, P. A. Boyle, L. L. Barnes, D. A. Bennett, and J. A. Schneider. 2020. "Limbic-Predominant Age-Related TDP-43 Encephalopathy, ADNC Pathology, and Cognitive Decline in Aging." *Neurology* 95, no. 14: e1951–e1962. https://doi.org/10.1212/WNL.0000000000010454.

Klöppel, S., A. Abdulkadir, C. R. Jack, N. Koutsouleris, J. Mourão-Miranda, and P. Vemuri. 2012. "Diagnostic Neuroimaging Across Diseases." *NeuroImage* 61: 457–463. https://doi.org/10.1016/j.neuroimage.2011.11.002.

Kotrotsou, A., D. A. Bennett, J. A. Schneider, et al. 2014. "Ex Vivo MR Volumetry of Human Brain Hemispheres." *Magnetic Resonance in Medicine* 71: 364–374. https://doi.org/10.1002/mrm.24661.

Kotrotsou, A., J. A. Schneider, D. A. Bennett, et al. 2015. "Neuropathologic Correlates of Regional Brain Volumes in a Community Cohort of Older Adults." *Neurobiology of Aging* 36: 2798–2805. https://doi.org/10.1016/j.neurobiolaging.2015.06.025.

Lamar, M., S. Leurgans, A. Kapasi, et al. 2022. "Complex Profiles of Cerebrovascular Disease Pathologies in the Aging Brain and Their Relationship With Cognitive Decline." *Stroke* 53, no. 1: 218–227. https://doi.org/10.1161/STROKEAHA.121.034814.

Lindberg, O., M. Walterfang, J. C. L. Looi, et al. 2012. "Hippocampal Shape Analysis in Alzheimer's Disease and Frontotemporal Lobar Degeneration Subtypes." *Journal of Alzheimer's Disease* 30: 355–365. https://doi.org/10.3233/JAD-2012-112210.

Luo, X., Q. Mao, J. Shi, X. Wang, and C. R. Li. 2019. "Putamen Gray Matter Volumes in Neuropsychiatric and Neurodegenerative Disorders." *World Journal of Psychiatry and Mental Health Research* 3, no. 1: 1020.

Makkinejad, N., J. A. Schneider, J. Yu, et al. 2019. "Associations of Amygdala Volume and Shape With Transactive Response DNA-Binding Protein 43 (TDP-43) Pathology in a Community Cohort of Older Adults." *Neurobiology of Aging* 77: 104–111. https://doi.org/10.1016/j.neurobiolaging.2019.01.022.

Mann, D. M. A. 1991. "The Topographic Distribution of Brain Atrophy in Alzheimer's Disease." *Acta Neuropathologica* 83: 81–86. https://doi.org/10.1007/BF00294434.

Marquié, M., M. Siao Tick Chong, A. Antón-Fernández, et al. 2017. "[F-18]-AV-1451 Binding Correlates With Postmortem Neurofibrillary Tangle Braak Staging." *Acta Neuropathologica* 134, no. 4: 619–628. https://doi.org/10.1007/s00401-017-1740-8.

McKeith, I. G., D. W. Dickson, J. Lowe, et al. 2005. "Diagnosis and Management of Dementia With Lewy Bodies: Third Report of the DLB Consortium." *Neurology* 65, no. 12: 1863–1872. https://doi.org/10.1212/01.wnl.0000187889.17253.b1.

McKhann, G., D. Drachman, M. Folstein, R. Katzman, D. Price, and E. M. Stadlan. 1984. "Clinical Diagnosis of Alzheimer's Disease: Report of the NINCDS-ADRDA Work Group Under the Auspices of Department of Health and Human Services Task Force on Alzheimer's Disease." *Neurology* 34: 939–944.

Miller, M. I., L. Younes, J. T. Ratnanather, et al. 2015. "Amygdalar Atrophy in Symptomatic Alzheimer's Disease Based on Diffeomorphometry: The BIOCARD Cohort." *Neurobiology of Aging* 36: S3–S10. https://doi.org/10.1016/j.neurobiolaging.2014.06.032.

Mirra, S. S., A. Heyman, D. McKeel, et al. 1991. "The Consortium to Establish a Registry for Alzheimer's Disease (CERAD). Part II. Standardization of the Neuropathologic Assessment of Alzheimer's Disease." *Neurology* 41, no. 4: 479–486. https://doi.org/10.1212/wnl.41.4.479.

Nag, S., L. Yu, P. A. Boyle, S. E. Leurgans, D. A. Bennett, and J. A. Schneider. 2018. "TDP-43 Pathology in Anterior Temporal Pole Cortex in Aging and Alzheimer's Disease." *Acta Neuropathologica Communications* 6, no. 1: 33. https://doi.org/10.1186/s40478-018-0531-3.

Nagy, Z., D. M. Yilmazer-Hanke, H. Braak, E. Braak, C. Schultz, and J. Hanke. 1998. "Assessment of the Pathological Stages of Alzheimer's Disease in Thin Paraffin Sections: A Comparative Study." *Dementia and Geriatric Cognitive Disorders* 9, no. 3: 140–144. https://doi.org/10.1159/000017038.

Nebel, R. A., N. T. Aggarwal, L. L. Barnes, et al. 2018. "Understanding the Impact of Sex and Gender in Alzheimer's Disease: A Call to Action." *Alzheimer's & Dementia: The Journal of the Alzheimer's Association* 14, no. 9: 1171–1183. https://doi.org/10.1016/j.jalz.2018.04.008.

Nelson, P. T., D. W. Dickson, J. Q. Trojanowski, et al. 2019. "Limbic-Predominant Age-Related TDP-43 Encephalopathy (LATE): Consensus Working Group Report." *Brain: A Journal of Neurology* 142, no. 6: 1503–1527. https://doi.org/10.1093/brain/awz099.

Nelson, P. T., G. A. Jicha, F. A. Schmitt, et al. 2007. "Clinicopathologic Correlations in a Large Alzheimer Disease Center Autopsy Cohort: Neuritic Plaques and Neurofibrillary Tangles 'Do Count' When Staging Disease Severity." *Journal of Neuropathology and Experimental Neurology* 66, no. 12: 1136–1146. https://doi.org/10.1097/nen.0b013e31815c5efb.

Nelson, P. T., E. B. Lee, M. D. Cykowski, et al. 2023. "LATE-NC Staging in Routine Neuropathologic Diagnosis: An Update." *Acta Neuropathologica* 145, no. 2: 159–173. https://doi.org/10.1007/s00401-022-02524-2.

Nie, X., Y. Sun, S. Wan, et al. 2017. "Subregional Structural Alterations in Hippocampus and Nucleus Accumbens Correlate With the Clinical Impairment in Patients With Alzheimer's Disease Clinical Spectrum: Parallel Combining Volume and Vertex-Based Approach." *Frontiers in Neurology* 8: 399. https://doi.org/10.3389/fneur.2017.00399.

Oppedal, K., D. Ferreira, L. Cavallin, et al. 2019. "A Signature Pattern of Cortical Atrophy in Dementia With Lewy Bodies: A Study on 333 Patients From the European DLB Consortium." *Alzheimer's & Dementia: The Journal of the Alzheimer's Association* 15, no. 3: 400–409. https://doi.org/10.1016/j.jalz.2018.09.011.

Orlhac, F., J. J. Eertink, A. S. Cottereau, et al. 2022. "A Guide to ComBat Harmonization of Imaging Biomarkers in Multicenter Studies." *Journal of Nuclear Medicine: Official Publication, Society of Nuclear Medicine* 63, no. 2: 172–179. https://doi.org/10.2967/jnumed.121.262464.

Pikkarainen, M., S. Rönkkö, V. Savander, R. Insausti, and A. Pitkänen. 1999. "Projections From the Lateral, Basal, and Accessory Basal Nuclei of the Amygdala to the Hippocampal Formation in Rat." *Journal of Comparative Neurology* 403, no. 2: 229–260.

Pitkänen, A., J. L. Kelly, and D. G. Amaral. 2002. "Projections From the Lateral, Basal, and Accessory Basal Nuclei of the Amygdala to the Entorhinal Cortex in the Macaque Monkey." *Hippocampus* 12, no. 2: 186–205. https://doi.org/10.1002/hipo.1099.

Price, J. L. 2003. "Comparative Aspects of Amygdala Connectivity." *Annals of the New York Academy of Sciences* 985: 50–58. https://doi.org/10.1111/j.1749-6632.2003.tb07070.x.

Qiu, A., C. Fennema-Notestine, A. M. Dale, and M. I. Miller. 2009. "Regional Shape Abnormalities in Mild Cognitive Impairment and Alzheimer's Disease." *NeuroImage* 45: 656–661. https://doi.org/10.1016/j.neuroimage.2009.01.013.

Roh, J. H., A. Qiu, S. W. Seo, et al. 2011. "Volume Reduction in Subcortical Regions According to Severity of Alzheimer's Disease." *Journal of Neurology* 258: 1013–1020. https://doi.org/10.1007/s00415-010-5872-1.

Scher, A. I., Y. Xu, E. S. C. Korf, et al. 2007. "Hippocampal Shape Analysis in Alzheimer's Disease: A Population-Based Study." *NeuroImage* 36: 8–18. https://doi.org/10.1016/j.neuroimage.2006.12.036.

Schneider, J. A., R. S. Wilson, E. J. Cochran, et al. 2003. "Relation of Cerebral Infarctions to Dementia and Cognitive Function in Older Persons." *Neurology* 60, no. 7: 1082–1088. https://doi.org/10.1212/01.wnl.0000055863.87435.b2.

Scott, S. A., S. T. DeKosky, and S. W. Scheff. 1991. "Volumetric Atrophy of the Amygdala in Alzheimer's Disease: Quantitative Serial Reconstruction." *Neurology* 41: 351–356. https://doi.org/10.1212/wnl.41.3.351.

Shi, F., B. Liu, Y. Zhou, C. Yu, and T. Jiang. 2009. "Hippocampal Volume and Asymmetry in Mild Cognitive Impairment and Alzheimer's Disease: Meta-Analyses of MRI Studies." *Hippocampus* 19: 1055–1064. https://doi.org/10.1002/hipo.20573.

Smith, S. M., M. Jenkinson, M. W. Woolrich, et al. 2004. "Advances in Functional and Structural MR Image Analysis and Implementation as FSL." *NeuroImage* 23, no. Suppl 1: S208–S219. https://doi.org/10.1016/j.neuroimage.2004.07.051.

Soontornniyomkij, V., M. D. Lynch, S. Mermash, et al. 2010. "Cerebral Microinfarcts Associated With Severe Cerebral Beta-Amyloid Angiopathy." *Brain Pathology (Zurich, Switzerland)* 20, no. 2: 459–467. https://doi.org/10.1111/j.1750-3639.2009.00322.x.

Strange, B. A., M. P. Witter, E. S. Lein, and E. I. Moser. 2014. "Functional Organization of the Hippocampal Longitudinal Axis." *Nature Reviews. Neuroscience* 15: 655–669. https://doi.org/10.1038/nrn3785.

Styner, M., I. Oguz, S. Xu, et al. 2006. "Framework for the Statistical Shape Analysis of Brain Structures Using SPHARM-PDM." *Insight Journal* 1071: 242–250. https://doi.org/10.54294/owxzil.

Tang, X., D. Holland, A. M. Dale, L. Younes, M. I. Miller, and Alzheimer's Disease Neuroimaging Initiative. 2014. "Shape Abnormalities of Subcortical and Ventricular Structures in Mild Cognitive Impairment and Alzheimer's Disease: Detecting, Quantifying, and Predicting." *Human Brain Mapping* 35, no. 8: 3701–3725. https://doi.org/10.1002/hbm.22431.

Teipel, S. J., H.-C. Fritz, and M. J. Grothe. 2020. "Neuropathologic Features Associated With Basal Forebrain Atrophy in Alzheimer Disease." *Neurology* 95: e1301. https://doi.org/10.1212/WNL.0000000000010192.

Thal, D. R., U. Rüb, M. Orantes, and H. Braak. 2002. "Phases of A Beta-Deposition in the Human Brain and Its Relevance for the Development of AD." *Neurology* 58, no. 12: 1791–1800. https://doi.org/10.1212/wnl.58.12.1791.

Valdés Hernández, M. D. C., S. R. Cox, J. Kim, et al. 2017. "Hippocampal Morphology and Cognitive Functions in Community-Dwelling Older People: The Lothian Birth Cohort 1936." *Neurobiology of Aging* 52: 1–11. https://doi.org/10.1016/j.neurobiolaging.2016.12.012.

van Veluw, S. J., K. Arfanakis, and J. A. Schneider. 2022. "Neuropathology of Vascular Brain Health: Insights From Ex Vivo Magnetic Resonance Imaging-Histopathology Studies in Cerebral Small Vessel Disease." *Stroke* 53, no. 2: 404–415. https://doi.org/10.1161/STROKEAHA.121.032608.

Vinters, H. V., W. G. Ellis, C. Zarow, et al. 2000. "Neuropathologic Substrates of Ischemic Vascular Dementia." *Journal of Neuropathology and Experimental Neurology* 59, no. 11: 931–945. https://doi.org/10.1093/jnen/59.11.931.

Visser, E., M. C. Keuken, G. Douaud, et al. 2016. "Automatic Segmentation of the Striatum and Globus Pallidus Using MIST: Multimodal Image Segmentation Tool." *NeuroImage* 125: 479–497. https://doi.org/10.1016/j.neuroimage.2015.10.013.

Whitwell, J. L., K. A. Josephs, M. E. Murray, et al. 2008. "MRI Correlates of Neurofibrillary Tangle Pathology at Autopsy: A Voxel-Based Morphometry Study." *Neurology* 71: 743–749. https://doi.org/10.1212/01.wnl.0000324924.91351.7d.

Whitwell, J. L., S. D. Weigand, M. M. Shiung, et al. 2007. "Focal Atrophy in Dementia With Lewy Bodies on MRI: A Distinct Pattern From Alzheimer's Disease." *Brain* 130, no. Pt 3: 708–719. https://doi.org/10.1093/brain/awl388.

Wilson, R. S., L. Yu, J. Q. Trojanowski, et al. 2013. "TDP-43 Pathology, Cognitive Decline, and Dementia in Old Age." *JAMA Neurology* 70, no. 11: 1418–1424. https://doi.org/10.1001/jamaneurol.2013.3961.

Winkler, A. M., G. R. Ridgway, M. A. Webster, S. M. Smith, and T. E. Nichols. 2014. "Permutation Inference for the General Linear Model." *NeuroImage* 92, no. 100: 381–397. https://doi.org/10.1016/j.neuroimage.2014.01.060.

Yi, H.-A., C. Möller, N. Dieleman, et al. 2016. "Relation Between Subcortical Grey Matter Atrophy and Conversion From Mild Cognitive Impairment to Alzheimer's Disease." *Journal of Neurology, Neurosurgery, and Psychiatry* 87: 425–432. https://doi.org/10.1136/jnnp-2014-309105.

Yoo, H. S., E. C. Lee, S. J. Chung, et al. 2020. "Effects of Alzheimer's Disease and Lewy Body Disease on Subcortical Atrophy." *European Journal of Neurology* 27, no. 2: 318–326. https://doi.org/10.1111/ene.14080.

Yushkevich, P. A., M. M. López, M. M. I. de Onzoño Martin, et al. 2021. "3D Mapping of Neurofibrillary Tangle Burden in the Human Medial Temporal Lobe." *bioRxiv*. https://doi.org/10.1101/2021.01.15.421909.

Supporting Information

Additional supporting information can be found online in the Supporting Information section.